HHS Public Access

Author manuscript

Cell Rep. Author manuscript; available in PMC 2016 June 16.

Published in final edited form as:

Cell Rep. 2015 June 16; 11(10): 1625–1637. doi:10.1016/j.celrep.2015.05.019.

ASXL2 regulates glucose, lipid and skeletal homeostasis

Takashi Izawa[1,*], **Nidhi Rohatgi**[1,*], **Tomohiro Fukunaga**[1], **Qun-Tian Wang**[2], **Matthew J. Silva**[3], **Michael J. Gardner**[3], **Michael L. McDaniel**[1], **Nada A. Abumrad**[4], **Clay F. Semenkovich**[5], **Steven L. Teitelbaum**[1,6,#], and **Wei Zou**[1,#]

[1]Department of Pathology and Immunology, Washington University School of Medicine, St. Louis, MO 63110

[2]Department of Biological Sciences, University of Illinois at Chicago, Chicago, IL 60607

[3]Department of Orthopedic Surgery, Washington University School of Medicine, St. Louis, MO 63110

[4]Division of Geriatrics and Nutritional Science, Department of Medicine, Washington University School of Medicine, St. Louis MO 63110

[5]Division of Endocrinology, Metabolism and Lipid Research, Department of Medicine, Washington University School of Medicine, St. Louis, MO 63110

[6]Division of Bone and Mineral Diseases, Department of Medicine, Washington University School of Medicine, St. Louis, MO 63110

Summary

ASXL2 is an ETP family protein that interacts with PPARγ. We find that ASXL2−/− mice are insulin resistant, lipodystrophic and fail to respond to a high fat diet. Consistent with genetic variation at the ASXL2 locus and human bone mineral density, ASXL2−/− mice are also severely osteopetrotic due to failed osteoclast differentiation attended by normal bone formation. ASXL2 regulates the osteoclast via two distinct signaling pathways. It induces osteoclast formation in a PPARγ/c-Fos-dependent manner and is required for RANK ligand- and thiazolidinedione-induced bone resorption, independent of PGC-1β. ASXL2 also promotes osteoclast mitochondrial

Contact information: Steven L. Teitelbaum, M.D., Washington University School of Medicine, Department of Pathology and Immunology, Campus Box 8118, 660 South Euclid Avenue, St. Louis, MO 63110, Phone: (314) 454-8463, Fax: (314) 454-5505, teitelbs@wustl.edu, Wei Zou, Ph.D., Washington University School of Medicine, Department of Pathology and Immunology, Campus Box 8118, 660 South Euclid Avenue, St. Louis, MO 63110, Phone: (314) 454-8463, Fax: (314) 454-5505, weizou@wustl.edu.

*These authors contributed equally to this work.

#These authors contributed equally to this work.

Author Contributions

T.I. designed and performed skeletal metabolic experiments. N.R. designed and performed dietary experiments and wrote manuscript. T.K. performed rosiglitazone bone experiments. Q-T. W. generated mice essential to study. M.J. S. designed fracture experiments. M.F.G. performed fracture experiments. M.L.M., N.A.A., and C.F.S. designed metabolic experiments. C.F.S. wrote manuscript. S.L.T. designed osteoclast bone experiment, supervised study, and wrote manuscript. W.Z. designed and performed experiment, supervised study, and wrote manuscript.

biogenesis in a process mediated by PGC-1β but independent of c-Fos. Thus, ASXL2 is a master regulator of skeletal, lipid and glucose homeostasis.

Graphical Abstract

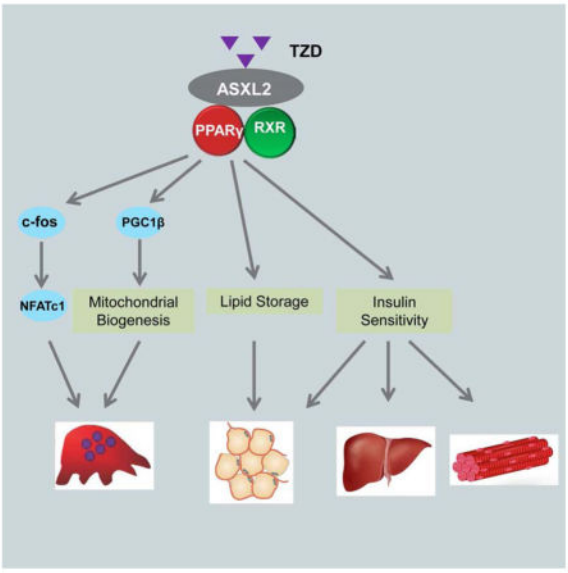

Introduction

The incidence of insulin resistant diabetes mellitus is probably the most rapidly increasing of any endemic disease in the United States. Obesity promotes type 2 diabetes (T2-DM), but not all obese individuals have diabetes, suggesting that the influence of genetic factors, particularly in specific ethnic groups, is substantial. T2-DM has skeletal complications. Diabetic patients are predisposed to fractures that heal poorly, in part because of compromised osteoclast function (de Liefde et al., 2005; Hernandez et al., 2012; Janghorbani et al., 2007; Kasahara et al., 2010; Vestergaard, 2007). Osteoclasts also probably contribute to the increased fracture incidence reported with TZD therapy (Kasahara et al., 2010; Lazarenko et al., 2007; Li et al., 2006; Sottile et al., 2004; Wan et al., 2007). Furthermore, recent evidence indicates the skeleton promotes glucose homeostasis via the osteoblast-specific protein, osteocalcin (Lee et al., 2007). The osteoclast is proposed to participate in this process by de-carboxylating osteocalcin and thus enabling it to stimulate pancreatic β-cells to produce insulin (Ferron et al., 2010).

We recently utilized genome wide screening to identify bone mineral density (BMD)-associated genes in mice (Farber et al., 2011) and found that the most significant BMD SNPs were in the ASXL2 gene. Establishing clinical relevance, SNPs within ASXL2 are associated with human BMD in two cohorts (Ghazalpour et al., 2012; Nielson et al., 2010).

ASXL2 is a mammalian homologue of the drosophila gene, ASX, which encodes an ETP protein, regulating histone methylation (Baskind et al., 2009). To gain insight into the means by which ASXL2 impacts the skeleton we performed gene cluster analysis (Farber et al.,

2011). Because we found the genes most prominently co-expressed with ASXL2 are those mediating myeloid differentiation, we postulated ASXL2 likely impacts the osteoclast, a member of the monocyte/macrophage family. In the present study, we find ASXL2−/− osteoclastogenesis is attenuated in vitro and in vivo. In keeping with a paucity of bone-resorptive cells, trabecular bone mass is increased more than 400% in mice lacking ASXL2.

PPARγ is a nuclear receptor that, in its unliganded state, is inactive due to association with co-repressing molecules (Tontonoz and Spiegelman, 2008). Upon ligand-induced activation, co-repressors disassociate and PPARγ recruits co-factors that enable transactivation of target genes. This nuclear receptor regulates insulin sensitivity and adipogenesis and can be involved in the pathogenesis of T2-DM. The preponderance of evidence indicates that fat is the primary tissue targeted by PPARγ to enhance insulin sensitivity where it promotes storage of dietary fatty acids in adipose tissues. Thiazolidinediones (TZDS), pharmacological activators of PPARγ, exert their insulin-sensitizing effects primarily by lowering free fatty acids.

TZDs, such as rosiglitazone (ROSI) have, until recently, enjoyed wide use in treating insulin resistance. Administration of these drugs is, however, restricted because of complications, including predisposition to fracture (Grey, 2009). Thus, the means by which activated PPARγ compromises the skeleton has important clinical implications.

PPARγ exerts its skeletal effects by impacting both osteoblasts and osteoclasts. In the case of osteoblasts, the nuclear receptor commits common precursor mesenchymal stem cells to differentiate into adipocytes at the cost of osteoblastogenesis, thereby reducing bone formation. PPARγ promotes osteoclast differentiation via activation of the osteoclastogenic AP-1 transcription factor, c-Fos (Wan et al., 2007). Thus, a reasonable hypothesis holds that TZD-mediated bone loss represents suppressed formation and enhanced resorption. In fact, enhanced resorption is the exclusive cause of ROSI-induced bone loss in mice (Fukunaga et al., 2015) and a component of the increased fracture risk in women (Zinman et al., 2010).

ASXL2 interacts with PPARγ and activates adipogenic genes (Park et al., 2011) raising the possibility ASXL2 may participate in the bone regulating effects of the nuclear receptor. We find that ASXL2 is necessary for cell autonomous osteoclastogenesis in a PPARγ/c-Fos-dependent manner. Thus, ASXL2 deficiency obviates the osteoclast-inducing capacity of ROSI. ASXL2 also promotes mitochondrial biogenesis in osteoclasts via PGC1-β in a manner independent of differentiation and c-Fos expression. Attesting to its cell specificity, ASXL2 does not regulate osteoblastic bone formation. Furthermore, ASXL2-deficient mice are lipodystrophic and relatively unresponsive to high fat diet (HFD). They have impaired glucose homeostasis and liver, fat, muscle and osteoclast precursors are insulin resistant. Thus, ASXL2 regulates skeletal, glucose and adipocyte homeostasis.

RESULTS

ASXL2 deficiency inhibits osteoclastogenesis

With the discovery that ASXL2 SNPs are associated with murine BMD, we knocked ASXL2 down in osteoclast precursors in the form of bone marrow macrophages (BMMs)

and discovered a marked arrest of osteoclastogenesis (Farber et al., 2011). To determine the physiological relevance of this observation, we cultured BMMs of ASXL2−/− mice in M-CSF and increasing amounts of the osteoclast differentiating cytokine, RANK ligand (RANKL). ASXL2-deficient osteoclast number is substantially reduced at all RANKL concentrations (Fig1A, S1A). Similarly, temporal expression of osteoclast differentiation markers is arrested in RANKL + M-CSF-exposed ASXL2−/− BMMs (Fig 1B, S1B). Reflecting reduced numbers of the bone resorptive cells, mobilization of CTx, a product of collagen degradation, is diminished in cultures of ASXL2−/− osteoclasts generated on bone (Fig 1C). Osteoclastogenesis of ASXL2+/− BMMs mirrors WT (not shown).

The fact that osteoclastogenesis of ASXL2−/− BMMs is dampened, in the absence of stromal cells or osteoblasts, suggests the influence of a mechanism endogenous to the osteoclast precursor (osteoclast autonomous). To determine if such is the case, we transduced ASXL2−/− BMMs with ASXL2 or empty vector. Likely because of construct size, transduction efficiency is less than optimal resulting in ASXL2 expression approximately 1/3 that of WT cells (Fig S1C). Despite this limitation, ASXL2 substantially, although incompletely, rescues osteoclast formation by mutant BMMs establishing a cell-autonomous influence (Fig 1D). In keeping with the partial rescue of the mutant cells by the WT construct, expression of the osteoclastogenic transcription factors, c-Fos and NFATc1 are significantly but modestly increased (Fig S1C). Because the partial rescue of ASXL2−/− osteoclastogenesis by ASXL2 transduction raised the possibility of a non-cell autonomous influence we generated various co-cultures of mutant and WT BMMs and osteoblasts in osteoclastogenic conditions. These experiments were based upon the fact that cytokines produced by osteoblast lineage cells are the key inducers of osteoclast differentiation. Consistent with diminished RANKL expression (Fig S1D), ASXL2−/− osteoblasts exert a modest negative influence on commitment of WT BMMs to the osteoclast phenotype (Fig 1E). Osteoclastogenesis, however, is virtually arrested when mutant BMMs are cultured with either WT or ASXL2-deficient osteoblasts. Thus, while RANKL production by ASXL2−/− osteoblast lineage cells is dampened, the deficiency does not contribute to the diminished number of mutant osteoclasts.

Exposure of BMMs to mesenchymal cell-produced RANKL, in vivo, primes them to differentiate into osteoclasts, ex vivo (Lam et al., 2000). To determine if ASXL2−/− osteoclast precursors respond to such priming, we transplanted WT or ASXL2−/− marrow in irradiated WT mice, a model in which all derivative osteoclasts, but not osteoblasts, are of donor origin (Lam et al., 2000). Marrow was obtained from the transplanted animals after 6 weeks and BMMs cultured in RANKL + M-CSF. BMMs of WT>WT chimeras generate abundant osteoclasts which are virtually absent when the cultured cells are obtained from marrow of ASXL2−/−>WT chimeras (Fig 1F). Thus, in keeping with the cell autonomous nature of the process, ASXL2−/− osteoclast precursors are resistant to priming by differentiation-inducing cytokines, in vivo.

ASXL2−/− mice are osteopetrotic

These observations establish that ASXL2 deficiency compromises osteoclast formation in a cell autonomous manner. Because osteopetrosis represents increased bone mass due to

compromised osteoclast formation and/or function, we measured bone mass of mutant mice by μCT. In fact, femoral trabecular bone mass (BV/TV) is increased approximately 400% in ASXL2−/− mice (Fig 1G). Trabecular connectivity, spacing and number exhibit equally impressive changes (Fig S1E). Histomorphometric analysis reveals the same abundance of trabecular bone mass and in keeping with our in vitro data, a significant decrease in osteoclast number (Fig 1H). Interestingly, while vertebral BV/TV is increased in absence of ASXL2, the change is relatively modest compared to appendicular bone. (Fig S1F). Similar to other osteopetrotic animals, cortical thickness is reduced eventuating in compromised bone strength (Fig S1G) (Li et al., 1999). As in human glucose intolerance (*vide infra*), fracture healing of ASXL2−/− mice is also retarded (Fig S1H).

Osteopetrosis is often associated with splenomegaly due to extramedullary hematopoiesis and ASXL2−/− mice have enlarged spleens ($p<0.01$). An abundance of megakaryocytes (not shown), taken with a paucity of bone marrow cells, establishes the splenomegaly of the mutant mice reflects extramedullary hematopoiesis (Fig S1I).

These data stand in contradistinction to our report of decreased BMD, as determined by DXA, in ASXL2−/− mice (Farber et al., 2011). DXA analysis is, however, modified by subject size and the results decrease in face of smaller bone, thus obviating meaningful interpretation in pediatric patients (Reid, 2010). In this regard, ASXL2−/− mice are smaller and weigh less than their WT counterparts (Fig 1I). The fact that the projected bone area of ASXL2−/− femurs is reduced approximately 1/3 (WT .96+/− .03mm^2; ASXL2−/− .67+/− .03mm^2; $p<.01$) explains the discrepancy between the substantially enhanced trabecular bone volume determined by μCT and the artifactually low BMD measured by DXA.

ASXL2 is abundantly expressed in osteoblasts (Farber et al., 2011). Thus, while our data establish ASXL2−/− mice are osteopetrotic, it is possible that, as in other forms of osteopetrosis, enhanced osteoblast activity may contribute to the increased bone mass (Marzia et al., 2000). ASXL2, however, does not appear to regulate bone formation since temporal expression of osteocalcin, bone sialoprotein, alkaline phosphatase and collagen 1 mRNA, by ASXL2−/− and WT cultured osteoblasts, is indistinguishable (Fig S1J). The same holds regarding in vivo osteoblast number and circulating osteocalcin (Fig 1H, S1K). Moreover, differentiation of marrow stromal cells into bone forming osteoblasts is unaltered in absence of ASXL2 (Fig S1L). To kinetically determine the impact of ASXL2 deletion on osteogenesis, we administered time-spaced doses of calcein and measured parameters of bone formation in non-decalcified sections. Mineral apposition (MAR) and bone formation (BFR) rates are the same in ASXL2−/− and WT animals (Fig 1H). Thus, ASXL2 deficiency increases bone mass by attenuating osteoclast formation without impacting osteoblasts.

PPARγ mediates ASXL2 stimulated osteoclastogenesis

Activated PPARγ promotes osteoclastogenesis and its absence, in BMMs, inhibits differentiation into mature bone resorbing cells (Wan et al., 2007). Furthermore, conditional deletion of the nuclear receptor, in hematopoietic and endothelial cells, increases bone mass (Wan et al., 2007). ASXL2 and PPARγ interact in other cells, raising the possibility the nuclear receptor may mediate ASXL2's osteoclastogenic capacity (Park et al., 2011). To test this hypothesis, we first asked if the ASXM2 domain of ASXL2, which is the binding site of

PPARγ's transcriptional partner, RXRα (Katoh, 2013), mediates osteoclast formation. In contrast to the induction of osteoclast differentiation markers by WT ASXL2, that lacking the ASXM2 domain is incapable of doing so in mutant BMMs (Fig S2A) (Relative mRNA expression: Vect=1; WT= 1.9; Delta ASXM2= 2.4). We next transfected 293T cells with a PPARγ luciferase reporter, with or without PPARγ (Fig 2A). Co-transfection with ASXL2 dose-dependently increases luciferase activity only in the presence of PPARγ (Fig 2A). Furthermore, ROSI, which therapeutically stimulates PPARγ in diabetic patients, synergistically enhances the capacity of ASXL2 to induce the PPARγ reporter construct. ROSI also substantially increases ASXL2/PPARγ association (Fig 2B). Further supporting its regulation of the nuclear receptor's osteoclastogenic effects, induction of the PPARγ target gene, CD36, requires ASXL2 (Fig 2C). ASXL2 also dampens PPARγ SUMOylation, a process which represses the nuclear receptor's transcriptional activity (van Beekum et al., 2009) (Fig 2D). Establishing a central role of ASXL2 in PPARγ-mediated osteoclast formation, induction of the bone resorptive polykaryon, by ROSI, is completely arrested in knockout cells (Fig 2E, S2B). On the other hand, ROSI-induced osteoclastogenesis does not reflect stimulated expression of ASXL2 by the TZD (Fig S2C) nor does ASXL2 deficiency affect PPARγ expression (Fig S2D). Thus, ASXL2 partners with ROSI to promote osteoclast formation via PPARγ activation.

c-Fos mediates ASXL2-induced osteoclastogenesis

ASXL2 is essential for RANKL-stimulated expression of the AP-1 transcription factor, c-Fos, deficiency of which completely arrests osteoclastogenesis, thereby promoting severe osteopetrosis (Fig 2F, S2E) (Grigoriadis et al., 1994). In keeping with c-Fos's essential role as an ASXL2 effector, transduction of the AP-1 protein rescues the osteoclastogenic capacity of ASXL2−/− BMMs (Fig 2G, 2H, S2F, S2G). Interestingly, c-Fos is a PPARγ target gene whose expression is enhanced in osteoclast precursors by ROSI (Wan et al., 2007). In fact, in the absence of ASXL2, PPARγ binding to its c-Fos response element does not increase with osteoclast differentiation, nor is it heightened by ROSI (Fig 2I).

RANK-stimulated osteoclast formation requires ASXL2

Differentiation of progenitors into mature osteoclasts is principally, if not exclusively, the purview of RANKL. In this regard, transduction the RANKL-induced, essential transcription factor, NFATc1, substantially rescues the osteoclastogenic capacity of ASXL2−/− BMMs (Fig 3A,B,C). Consistent with c-Fos being upstream of NFATc1 in osteoclastogenesis, transduction of NFATc1 does not increase c-Fos expression in ASXL2−/− osteoclasts (Fig 3D). It therefore appears that the impaired osteoclastogenesis of ASXL2−/− BMMs reflects failed activation of the RANKL canonical signaling pathway. In fact, RANKL-stimulated cytoplasmic and nuclear osteoclastogenic signals are compromised in ASXL2−/− cells (Fig 3E, F). Furthermore, RANK expression by BMMs and pre-fusion osteoclasts is diminished in the absence of ASXL2 (Fig 3G).

These observations suggest that normal expression of RANK, when activated, is necessary and may be sufficient to mediate ASXL2-stimulated osteoclast formation. Such being the case, activated RANK should rescue the ASXL2−/− osteoclast phenotype. To confirm this notion, we expressed a protein consisting of the transmembrane and cytosolic domains of

RANK fused to the external domain of human Fas receptor (hFas/RANK) (Izawa et al., 2012). When exposed to anti-hFas antibody, WT macrophages bearing this construct differentiate into osteoclasts (Fig 3H). ASXL2−/− BMMs, however, fail to do so. This observation is in keeping with the failure of RANKL abundance to influence differentiation of ASXL2−/− osteoclast precursors (Fig 1E, S1D). Thus, even in the presence of activated RANK, ASXL2 is necessary for the osteoclastogenic process.

c-Fos expression is central to the means by which activated RANK promotes osteoclast formation. Because ASXL2 is also required for c-Fos expression we asked if the inability of hFas/RANK to rescue the mutant cells reflects failure to induce the AP-1 transcription factor and we find such to be the case (Fig 3I). Thus, the osteoclastogenic properties of RANK require ASXL2, which is essential for expression of the RANKL receptor, as well as c-Fos.

ASXL2 promotes PGC-1β expression and osteoclastogenic activity

Like PPARγ, its co-activator, PGC-1β, is essential for osteoclastogenesis, in vitro (Ishii et al., 2009). Given the functional relationship between PPARγ and PGC-1β, we asked if the latter participates in ASXL2's osteoclastogenic properties. Unlike the stable expression of ASXL2 (Fig S2C), PGC-1β progressively increases during osteoclastogenesis in an ASXL2-dependent manner (Fig 4A,B). In fact, absence of ASXL2 obviates both basal and ROSI-stimulated PGC-1β expression during osteoclast differentiation. (Fig 4A,B,C). Furthermore, ASXL2 localizes with PGC-1β on the retinoic acid response element, a process mediated by PPARγ activation as evidenced by the stimulatory effect of ROSI (Fig 4D).

PGC-1β is proposed to impact the osteoclast by two distinct yet integrated pathways. First, by activating PPARγ, PGC-1β is believed to participate in c-Fos induction (Wei et al., 2010). Second, PGC-1β, when reciprocally induced by activated PPARγ, promotes mitochondrial biogenesis, considered necessary for osteoclast differentiation and/or function (Ishii et al., 2009; Wei et al., 2010). To determine if ASXL2 regulates generation of osteoclast mitochondria, we treated mutant and WT BMMs with various combinations of RANKL +/− ROSI. Mitochondrial enzyme mRNA abundance was determined after 3 days. Consistent with the copious mitochondria characterizing mature osteoclasts, basal- and ROSI- induced enzyme mRNA expression is blunted in cells lacking ASXL2 (Fig 4E). Thus, ASXL2 is necessary for normal mitochondrial biogenesis, which is augmented by activated PPARγ.

Given its central role in osteoclast mitochondrial biogenesis, we next asked if PGC-1β mediates ASXL2's effects on the process. Thus, we transduced ASXL2−/− BMMs with PGC-1β and exposed them to M-CSF +/− RANKL. PGC-1β completely normalizes mitochondrial enzyme expression by ASXL2−/− osteoclast lineage cells (Fig 4F). Surprisingly, however, PGC-1β does not rescue the failure of ASXL2-deficient BMMs to commit to the osteoclast phenotype and is actually suppressive, as evidenced by decreased cathepsin K (Fig 4G). This observation raised the possibility that PGC-1β does not induce essential osteoclastogenic transcription factors such as c-Fos. To determine if this is so, we transduced ASXL2−/− BMMs with c-Fos or PGC-1β. Vector-bearing ASXL2−/− cells served as control. The cells were cultured for 24 hours in M-CSF, with or without RANKL. Despite robust expression of transduced c-Fos and PGC-1β, each fails to enhance mRNA of

the other in ASXL2−/− BMMs or pre-fusion osteoclasts (pOCs) (Fig 4H). In fact, PGC-1β actually diminishes c-Fos mRNA abundance. Furthermore, while PGC-1β rescues expression of the 5 principal eukaryotic mitochondrial enzyme complexes (OXPHOS proteins) in ASXL2−/− BMMs and/or pOCs, c-Fos has no such effect (Fig 4I). Hence, PGC-1β and mitochondrial biogenesis, together, are insufficient to promote ASXL2−/− osteoclast formation as they do not induce c-Fos nor the osteoclast-specific protein, cathepsin K. Similarly, c-Fos fails to induce PGC-1β expression or mitochondrial biogenesis. These observations suggest ASXL2 regulates two distinct pathways in osteoclasts. The first involves PGC-1β-stimulated energy metabolism, which mediates the mature cell's capacity to degrade bone, while the second involves c-Fos promotion of osteoclast differentiation.

ASXL2 does not suppress key PPARγ co-repressors

These data indicate ASXL2 likely promotes osteoclastogenesis in association with transactivation of PGC-1β, a PPARγ co-activator. They do not, however, exclude the possibility that ASXL2 also exerts its osteoclastogenic effects by suppressing transcription of a PPARγ co-repressor(s). This hypothesis is in keeping with the fact that ASXL2 is an ETP protein that regulates histone 3 methylation to establish repressive or active chromatin configurations at target loci (Baskind et al., 2009). Indicating ASXL2 does not suppress PPARγ co-repressors, the mRNA abundance of 2 such key inhibitors, NCoR and SMRT does not increase in the absence of the ETP protein (Yu et al., 2005) (Fig S3). Thus, the osteoclastogenic properties of ASXL2 are mediated by activating PPARγ and probably not by inhibiting its repression.

ASXL2 deficiency promotes insulin resistance and glucose intolerance

PPARγ plays a central role in insulin sensitivity. Because ASXL2 activates PPARγ in the osteoclastogenic process, we postulated ASXL2 may also promote glucose homeostasis. In fact, ASXL2−/− mice are glucose intolerant (Fig 5A). Consistent with this condition, basal serum glucose is increased in fasting and fed states (Fast- WT 65.4 +/− 11.4; ASXL2 −/− 112.6 +/− 18.4; Fed- WT 118.7 +/−15.26; ASXL2−/− 170.75 +/− 31.82; mg/dl +/−SD $p<0.01$). On the other hand and typical of early onset T2-DM, their circulating basal insulin is normal (WT .31+/− .10; ASXL2−/− .32+/− .17; ng/ml +/−SD). Asxl2-deficient mice also exhibit attenuated clearance of glucose following insulin challenge (Fig 5B). Insulin resistance in ASXL2-deficient mice is further substantiated by the inability of Iiver and muscle to phosphorylate Akt or the insulin receptor in response to in vivo insulin administration (Fig 5C,D). The mice also exhibit increased hepatic expression of the gluconeogenic enzymes, glucose-6-phosphatase and phosphoenolpyruvate carboxykinase (Fig 5E). The role of PPARγ in ASXL2−/− extraskeletal insulin resistance is supported by suppressed expression of CD36 in mutant liver, fat and muscle (Fig 5F) (Hu et al., 2012). Thus, ASXL2 deficiency produces a state of insulin-resistant glucose intolerance in conjunction with failed osteoclastogenesis and osteopetrosis.

ASXL2 does not regulate glucose metabolism via its expression in osteoclasts

Osteoclasts may participate in the pathogenesis of murine diabetes (Ferron et al., 2010). To determine if ASXL2-deficiency in the bone resorptive cell modifies glucose homeostasis,

we transplanted WT or ASXL2−/− marrow into irradiated WT mice (Lam et al., 2000). Despite the fact that transplantation of the mutant marrow into irradiated WT mice, yields the ASXL2−/− osteoclast phenotype (Fig 1F), glucose tolerance remains normal as it mirrors that of WT to WT transplantation (Fig 5G). Thus, in contrast to murine T1-DM in which osteoclast dysfunction might be pathogenic (Ferron et al., 2010), the resorptive cell's abnormalities do not appear to contribute to systemic insulin resistance in ASXL2 deficiency.

ASXL2-mediated insulin sensitivity does not regulate osteoclastogenesis

ASXL2−/− BMMs are also insulin resistant as evidenced by diminished InR, Akt and S6(S235/236) phosphorylation in response to the hormone (Fig 5H,I,J). As BMMs are osteoclast precursors, this observation suggests their insulin insensitivity may contribute to the attenuated osteoclastogenesis attending ASXL2 deficiency. To determine if insulin signaling in osteoclast precursors is necessary for the osteoclastogenic process, we deleted the InR in $InR^{fl/fl}$ BMMs, with retroviral Turbo-cre (Bai et al., 2008). As seen in (Fig S4A,B) absence of the InR does not alter differentiation of osteoclast precursors. Thus, failure of ASXL2-deficient osteoclast formation does not reflect insulin insensitivity of precursors.

ASXL2−/− mice are lipodystrophic

PPARγ is required for adipogenesis and its absence produces a lipodystrophic state. Similarly, ASXL2 overexpression in 3T3-L1 pre-adipocytes transactivates adipogenic genes (Park et al., 2011). In consequence, ASXL2−/− mice are partially lipodystrophic as manifested by decreased abundance of epididymal (eWAT) and subcutaneous (scWAT) white and brown (BAT) adipose tissue as well as DXA-determined fat/lean ratio (Fig 6A,B; S5A,B). Despite the paucity of fat, VO_2 is only slightly decreased and exclusively in light cycle (Fig S5C). Likewise, respiratory quotient (RQ) of ASXL2−/− mice mirrors that of WT. These data suggest ASXL2−/− and WT mice enjoy similar use of fuels as energy source.

ASXL2−/− adipocytes are insulin insensitive as they fail to optimally phosphorylate Akt^{308} in response to the hormone (Fig 6C). Mirroring cells in which PPARγ is inactive, ASXL2-deficient adipocytes are small and their abundance is diminished (Fig 6D,E; S5D,E). Histological analysis of BAT and expression of the thermogenic marker, UCP1, remains unchanged in eWAT and BAT suggesting beiging of WAT does not induce the small adipocytes of ASXL2-deficiency (Fig S5F,G). Unlike cells in muscle and liver ASXL2−/− adipocytes normally phosphorylate their InR (Fig S5H). On the other hand, expression of adiponectin and leptin by adipocyte is reduced attesting to insulin insensitivity and the lipodystrophic phenotype (Fig 6F). Confirming compromised adipogenic capacity, differentiation of ASXL2−/− marrow stromal cells into fat is arrested (Fig 6G). Similarly, shRNA knockdown of ASXL2 reduces lipid accumulation in NIH3T3-L1 cells, corroborating the cell-autonomous nature of the process (Fig S5I). Additionally, C/EBPα mRNA whose product regulates leptin and PPARγ expression and promotes osteoclast formation (Chen et al., 2013) is reduced in ASXL2−/− fat (Fig 6F). The same holds regarding mRNA for AP2, CD36 (both induced by PPARγ) and solute carrier family 25,

member 1 (slc25a1). In contrast to these proteins, which promote maturation of differentiating adipocytes, expression of C/EBPβ, which stimulates earlier, pre-adipocyte maturation, is increased.

ASXL2 deletion does not affect glycerol mobilization even in presence of isoproterenol-induction indicating that the attendant paucity of fat is not due to enhanced lipolysis (Fig 6H). On the other hand, proteins, which mediate lipid storage, including fatty acid synthase (Fasn), Acetyl-CoA carboxylase 1 (Acaca), malic enzyme 1 (Me1) and Glut 4 are diminished in ASXL2−/− WAT (FIG 6I). In keeping with failure to store lipids, circulating triglycerides and cholesterol are increased in ASXL2-deficient mice (Fig 6J). Despite compromised lipid storage, liver and muscle fat are not enhanced in the mutant mice (Fig S5J,K,L). Thus, the lipodystrophic state of ASXL2−/− mice likely reflects defective lipid storage and not enhanced lipolysis.

ASXL2-deficient mice resist high fat diet

Obesity promotes insulin resistance suggesting that compromised adipogenesis may be protective in this regard. To determine if such is the case we fed WT and ASXL2−/− mice a HFD for 7 weeks. As expected WT mice gain substantial weight. In contrast, ASXL2-deficient animals fail to increase body mass despite similar food consumption (Fig 7A,B). Hence, the fat/lean ratio, as determined by DXA, remains low in HFD-fed ASXL2−/− mice (Fig 7C). While there is no discernable difference in marrow adipose tissue in chow fed animals, there is substantially less in the pair of femurs obtained from ASXL2−/− HFD mice (Table S1).

As expected, the metabolic phenotype is exacerbated in WT animals by HFD (Fig 7D,E,F). Chow fed ASXL2−/− mice are insulin resistant based on glucose and insulin tolerance tests, but this condition is not exacerbated by HFD. Lipokine levels reflect the expected physiology in WT mice with increases in leptin and decreases in adiponectin (Fig 7F), but these changes are substantially blunted in ASXL2−/− mice. This robust difference is consistent with the complex lipodystrophic phenotype of these mice and highlights the critical role of ASXL2 in the integrative physiology of lipid, glucose and skeletal metabolism.

Discussion

Our exploration of ASXL2 was prompted by its association with BMD in mice and man (Farber et al., 2011; Ghazalpour et al., 2012; Nielson et al., 2010). Because ASXL2 expression is linked to genes regulating myeloid differentiation, we suspected its skeletal effects are mediated via the osteoclast. In fact, both knockdown of ASXL2 and its absence in osteoclast precursors markedly arrest the osteoclastogenic process. Mirroring these in vitro experiments, the number of osteoclasts in ASXL2−/− mice is substantially reduced and ASXL2−/− mice are osteopetrotic. These animals also manifest systemic insulin resistance. These observations suggest that ASXL2 may participate in the complex relationship between skeletal biology and metabolism manifest in obesity-related diabetes.

Osteoclast formation may be regulated in a cell-autonomous (i.e. endogenous to the osteoclast) or non-autonomous manner. Non-autonomous osteoclastogenesis typically involves altered secretion of the key osteoclastogenic cytokines, RANKL and M-CSF by non-osteoclastic cells such as those of mesenchymal or T-cell lineage. Despite compromised RANKL expression by mutant osteoblasts, our observation that pure populations of ASXL2−/− BMMs fail to normally differentiate into osteoclasts indicated ASXL2's effects are principally cell autonomous. On the other hand, the magnitude of priming BMMs by RANKL, in vivo, may affect their subsequent capacity to commit to the osteoclast phenotype (Lam et al., 2000). The fact that the WT construct substantially rescues ASXL2−/− osteoclastogenesis that, in turn, is induced by transplantation of mutant marrow into irradiated WT mice, substantiates ASXL2's osteoclast autonomous nature.

Our conjecture that the osteoclastogenic effects of PPARγ require ASXL2 was prompted by the observation that the two nuclear proteins interact (Park et al., 2011). The essential role ASXL2 plays in PPARγ-induced osteoclast formation is established by ASXL2 being necessary for basal and TZD-stimulated activation of a PPARγ reporter construct. ASXL2 also promotes binding of PPARγ to its c-Fos response element and most importantly, is essential for expression of c-Fos and NFATc1. These observations indicate that the attenuated osteoclastogenesis attending ASXL2 deficiency reflects failure to express these TZD-induced transcription factors. Establishing this case, transduction of c-Fos or NFATc1 in ASXL2−/− BMMs promotes their differentiation into osteoclasts.

Osteoblasts and adipocytes have a common mesenchymal precursor and therefore their differentiation is competitive (Wan, 2010). PPARγ plays a central role in this selection as its activation promotes adipogenesis at the cost of the osteoblast. Based on the abundance of ASXL2 in osteoblasts, we expected its deficiency would enhance bone formation, contributing to the marked increase in trabecular bone volume. By this scenario, ASXL2 deficiency would obviate the pro-adipogenic effects of PPARγ, thereby encouraging osteoblast differentiation of their common precursor. Our in vitro and in vivo data establish such is not the case as multiple parameters of bone formation, including osteocalcin are unaltered in ASXL2−/− mice. Interestingly, the metabolic characteristics of ASXL2−/− mice, which have normal circulating osteocalcin and insulin, differ from those deficient in the osteoblast-specific protein. For example, lack of osteocalcin promotes obesity (Lee et al., 2007). In contrast, fat mass and adipocyte differentiation of ASXL2−/− mice are diminished, likely reflecting relatively late arrest of the adipogenic process and lipid storage. Thus, regulation of glucose homeostasis by osteocalcin and ASXL2 mechanistically differ. Whereas decreased osteocalcin principally compromises insulin production, absence of ASXL2 results in insulin resistance. Furthermore, despite evidence indicating the osteoclast participates in osteocalcin-mediated glucose homeostasis (Ferron et al., 2010), WT marrow transplanted into ASXL2−/− mice fails to rescue their diabetic state. Thus, while bone and glucose metabolism are each mediated by PPARγ, the effects of ASXL2 on the two events appear to be physiologically distinct. Our demonstration that, unlike ROSI, a TZD with impaired recognition of PPARγ (Chen et al., 2012) fails to promote osteoclast formation, provides credence to the concept that insulin sensitivity of BMMs does not impact their osteoclastogenic potential (Fukunaga et al., 2015).

The activity of PPARγ is dictated by ligand-induced disassociation of co-repressors and recruitment of co-stimulatory molecules. The varied distribution of PPARγ co-activators likely dictates tissue specificity of the nuclear receptor's transcriptional effects (Ahmadian et al., 2013). PGC-1β is believed to be a prevalent PPARγ co-activator in the osteoclastogenic process. Its expression is enhanced during osteoclast differentiation and its deletion arrests formation of the bone resorptive cell, in vitro, particularly when induced by ROSI (Ishii et al., 2009; Wei et al., 2010). Because ASXL2 exerts its osteoclastogenic effects in conjunction with PPARγ we asked if PGC-1β participates in the process. Mirroring the effects of PPARγ deletion, absence of ASXL2 completely obviates PGC-1β expression both basally and when induced by ROSI.

Dysfunctional mitochondrial biogenesis is central to the pathogenesis of insulin-resistant DM (Petersen et al., 2003; Vianna et al., 2006). This mitochondrial dysfunction is mediated by PGC-1α and its closest homologue, PGC-1β. While overexpression of either increases mitochondrial respiration in cultured cells, they are non-compensatory as deletion of either promotes a robust phenotype and selectively alters gene expression (Lin et al., 2004; Sonoda et al., 2007). This event is of particular significance in osteoclasts that, because of profound energy consumption, are extremely rich in mitochondria whose generation requires PGC-1β. In fact, absence of PGC-1β arrests the bone resorptive function of mature osteoclasts, in vivo (Ishii et al., 2009). However, the relative importance of PGC-1β and its induction of mitochondrial biogenesis to osteoclast formation was unknown.

Similar to PGC-1β, absence of ASXL2 diminishes basal and stimulated mitochondrial biogenesis. However, unlike c-Fos or NFATc1, which rescue the ASXL2−/− osteoclast phenotype, reconstitution with PGC-1β has no effect on differentiation of the mutant cells. These observations are consistent with the fact that while PGC-1β−/− osteoclast number is diminished, in vitro, it is normal, in vivo, but function of the cell is disturbed (Ishii et al., 2009). In a physiological context, therefore, PGC-1β and by association mitochondrial biogenesis, likely exert their effects by enabling resorptive activity and not by promoting osteoclast differentiation.

Arrest of differentiation-induced expression of RANK and its effector osteoclastogenic signals, provided a candidate mechanism for failure to optimally form the bone resorbing cells, in the absence of ASXL2. Thus, it was surprising that normalization of RANK does not increase c-Fos which when transduced into ASXL2−/− BMMs, rescues their osteoclast-poor phenotype. PGC-1β transduction, which promotes mitochondrial biogenesis, also fails to induce c-Fos or osteoclast formation in ASXL2−/− cells. Thus, regardless of agonist, osteoclastogenesis requires c-Fos which in turn, requires ASXL2. We propose that in contradistinction to PGC-1β, which via mitochondrial biogenesis, directly facilitates bone resorption, the primary osteoclastic effect of c-Fos, which does not enhance PGC-1β expression or mitochondrial biogenesis, is maturation with increased bone degradation being a secondary consequence. Thus, ASXL2 regulates osteoclast formation and function, respectively, by two distinct signaling pathways.

The role of ASXL2 in skeletal, glucose and lipid homeostasis establishes that this particular gene regulates all three systems. On the other hand, the products of ASXL2-mediated

regulation, such as osteoclastogenesis and insulin sensitivity, appear to be independent events that do not mutually impact each other. Thus, murine ASXL2 insufficiency predisposes to lipodystrophy, insulin-resistance and attendant skeletal dysfunction raising the possibility that ASXL2 may affect similar endpoints in people.

Experimental Procedures

Detailed information is available in the Supplemental Experimental Procedures.

Mice

ASXL2+/− mice (C57BL background and S129 background) were described previously (Baskind et al., 2009). To generate ASXL2−/− mice, C57BL ASXL2+/− mice were mated with S129 ASXL2+/− mice, F1 offspring were used for all experiments. Mice were housed in the animal care unit of Washington University School of Medicine, where they were maintained according to guidelines of the Association for Assessment and Accreditation of Laboratory Animal Care. All animal experimentation was approved by the Animal Studies Committee of Washington University School of Medicine.

Statistics

Statistical significance was determined using Student's *t* test. Data are expressed as mean +/− S.D. * $p<0.05$, ** $p<0.01$, *** $p<0.001$ in all experiments.

Supplementary Material

Refer to Web version on PubMed Central for supplementary material.

Acknowledgments

This work was supported by National Institutes of Health grants DK076729, DK56341 and DK20579 (CFS), 5R01AR050211 (MJS), 5R01AR03278828, 5R01AR05703705 and 5R37AR04652315 (SLT), P30AR057235, and P30DK056341 and Shriners Hospitals for Children grant 85400-STL (SLT). The authors wish to thank Evan Buettmann, Tarpit Patel, Soumya Ravindran, and Jean Chappel. We thank Thomas L. Clemens for providing $InR^{flox/flox}$ bones and Gerard Karsenty for reviewing the manuscript

References

Ahmadian M, Suh JM, Hah N, Liddle C, Atkins AR, Downes M, Evans RM. PPAR gamma signaling and metabolism: the good, the bad and the future. Nat Med. 2013; 19:557–566. [PubMed: 23652116]

Bai S, Kopan R, Zou W, Hilton MJ, Ong CT, Long F, Ross FP, Teitelbaum SL. NOTCH1 regulates osteoclastogenesis directly in osteoclast precursors and indirectly via osteoblast lineage cells. J Biol Chem. 2008; 283:6509–6518. [PubMed: 18156632]

Baskind HA, Na L, Ma Q, Patel MP, Geenen DL, Wang QT. Functional conservation of Asxl2, a murine homolog for the Drosophila enhancer of trithorax and polycomb group gene Asx. PLoS ONE. 2009; 4:e4750. [PubMed: 19270745]

Chen W, Zhu G, Hao L, Wu M, Ci H, Li YP. C/EBPalpha regulates osteoclast lineage commitment. Proceedings of the National Academy of Sciences U S A. 2013; 110:7294–7299.

Chen Z, Vigueira PA, Chambers KT, Hall AM, Mitra MS, Qi N, McDonald WG, Colca JR, Kletzien RF, Finck BN. Insulin resistance and metabolic derangements in obese mice are ameliorated by a

novel peroxisome proliferator-activated receptor gamma-sparing thiazolidinedione. J Biol Chem. 2012; 287:23537–23548. [PubMed: 22621923]

de Liefde I, van der Klift M, de Laet C, van Daele P, Hofman A, Pols H. Bone mineral density and fracture risk in type-2 diabetes mellitus: the Rotterdam Study. Osteoporos Int. 2005; 16:1713–1720. [PubMed: 15940395]

Farber CR, Bennett BJ, Orozco L, Zou W, Lira A, Kostem E, Kang HM, Furlotte N, Berberyan A, Ghazalpour A, Suwanwela J, Drake TA, Eskin E, Wang QT, Teitelbaum SL, Lusis AJ. Mouse genome-wide association and systems genetics identify Asxl2 as a regulator of bone mineral density and osteoclastogenesis. PLoS Genet. 2011; 7:e1002038. [PubMed: 21490954]

Ferron M, Wei J, Yoshizawa T, Del Fattore A, DePinho RA, Teti A, Ducy P, Karsenty G. Insulin signaling in osteoblasts integrates bone remodeling and energy metabolism. Cell. 2010; 142:296–308. [PubMed: 20655470]

Fukunaga T, Zou W, Rohatgi N, Colca JR, Teitelbaum SL. An insulin-sensitizing thiazolidinedione, which minimally activates PPARgamma, does not cause bone loss. J Bone Miner Res. 2015; 30:481–488. [PubMed: 25257948]

Ghazalpour A, Rau CD, Farber CR, Bennett BJ, Orozco LD, van Nas A, Pan C, Allayee H, Beaven SW, Civelek M, Davis RC, Drake TA, Friedman RA, Furlotte N, Hui ST, Jentsch JD, Kostem E, Kang HM, Kang EY, Joo JW, Korshunov VA, Laughlin RE, Martin LJ, Ohmen JD, Parks BW, Pellegrini M, Reue K, Smith DJ, Tetradis S, Wang J, Wang Y, Weiss JN, Kirchgessner T, Gargalovic PS, Eskin E, Lusis AJ, LeBoeuf RC. Hybrid mouse diversity panel: a panel of inbred mouse strains suitable for analysis of complex genetic traits. Mamm Genome. 2012; 23:680–692. [PubMed: 22892838]

Grey A. Thiazolidinedione-induced skeletal fragility--mechanisms and implications. Diabetes Obes Metab. 2009; 11:275–284. [PubMed: 18671797]

Grigoriadis AE, Wang ZQ, Cecchini MG, Hofstetter W, Felix R, Fleisch HA, Wagner EF. c-Fos: a key regulator of osteoclast-macrophage lineage determination and bone remodeling. Science. 1994; 266:443–448. [PubMed: 7939685]

Hernandez RK, Do TP, Critchlow CW, Dent RE, Jick SS. Patient-related risk factors for fracture-healing complications in the United Kingdom General Practice Research Database. Acta orthopaedica. 2012; 83:653–660. [PubMed: 23140093]

Hu S, Yao J, Howe AA, Menke BM, Sivitz WI, Spector AA, Norris AW. Peroxisome proliferator-activated receptor gamma decouples fatty acid uptake from lipid inhibition of insulin signaling in skeletal muscle. Mol Endocrinol. 2012; 26:977–988. [PubMed: 22474127]

Ishii KA, Fumoto T, Iwai K, Takeshita S, Ito M, Shimohata N, Aburatani H, Taketani S, Lelliott CJ, Vidal-Puig A, Ikeda K. Coordination of PGC-1beta and iron uptake in mitochondrial biogenesis and osteoclast activation. Nat Med. 2009; 15:259–266. [PubMed: 19252502]

Izawa T, Zou W, Chappel JC, Ashley JW, Feng X, Teitelbaum SL. c-Src links a RANK/alphavbeta3 integrin complex to the osteoclast cytoskeleton. Mol Cell Biol. 2012; 32:2943–2953. [PubMed: 22615494]

Janghorbani M, Van Dam RM, Willett WC, Hu FB. Systematic review of type 1 and type 2 diabetes mellitus and risk of fracture. Am J Epidemiol. 2007; 166:495–505. [PubMed: 17575306]

Kasahara T, Imai S, Kojima H, Katagi M, Kimura H, Chan L, Matsusue Y. Malfunction of bone marrow-derived osteoclasts and the delay of bone fracture healing in diabetic mice. Bone. 2010; 47:617–625. [PubMed: 20601287]

Katoh M. Functional and cancer genomics of ASXL family members. Br J Cancer. 2013; 109:299–306. [PubMed: 23736028]

Lam J, Takeshita S, Barker JE, Kanagawa O, Ross FP, Teitelbaum SL. TNF-alpha induces osteoclastogenesis by direct stimulation of macrophages exposed to permissive levels of RANK ligand. J Clin Invest. 2000; 106:1481–1488. [PubMed: 11120755]

Lazarenko OP, Rzonca SO, Hogue WR, Swain FL, Suva LJ, Lecka-Czernik B. Rosiglitazone induces decreases in bone mass and strength that are reminiscent of aged bone. Endocrinology. 2007; 148:2669–2680. [PubMed: 17332064]

Lee NK, Sowa H, Hinoi E, Ferron M, Ahn JD, Confavreux C, Dacquin R, Mee PJ, McKee MD, Jung DY, Zhang Z, Kim JK, Mauvais-Jarvis F, Ducy P, Karsenty G. Endocrine regulation of energy metabolism by the skeleton. Cell. 2007; 130:456–469. [PubMed: 17693256]

Li M, Pan LC, Simmons HA, Li Y, Healy DR, Robinson BS, Ke HZ, Brown TA. Surface-specific effects of a PPARgamma agonist, darglitazone, on bone in mice. Bone. 2006; 39:796–806. [PubMed: 16759917]

Li YP, Chen W, Liang Y, Li E, Stashenko P. Atp6i-deficient mice exhibit severe osteopetrosis due to loss of osteoclast-mediated extracellular acidification. Nat Genet. 1999; 23:447–451. [PubMed: 10581033]

Lin J, Wu PH, Tarr PT, Lindenberg KS, St-Pierre J, Zhang CY, Mootha VK, Jager S, Vianna CR, Reznick RM, Cui L, Manieri M, Donovan MX, Wu Z, Cooper MP, Fan MC, Rohas LM, Zavacki AM, Cinti S, Shulman GI, Lowell BB, Krainc D, Spiegelman BM. Defects in adaptive energy metabolism with CNS-linked hyperactivity in PGC-1alpha null mice. Cell. 2004; 119:121–135. [PubMed: 15454086]

Marzia M, Sims NA, Voit S, Migliaccio S, Taranta A, Bernardini S, Faraggiana T, Yoneda T, Mundy GR, Boyce BF, Baron R, Teti A. Decreased c-Src expression enhances osteoblast differentiation and bone formation. J Cell Biol. 2000; 151:311–320. [PubMed: 11038178]

Nielson C, Estrada K, Klein R, Rivadeneira F, Uitterlinden A, Orwoll E. Mouse QTL-directed Analysis of Homologous Human Chromosomal Regions in a Large Scale Meta-analysis of Genome-wide Association Studies of the GEFOS Consortium Reveals Novel Genetic Associations with Bone Mineral Density. J Bone Miner Res. 2010; 25(Suppl 1)

Park UH, Yoon SK, Park T, Kim EJ, Um SJ. Additional sex comb-like (ASXL) proteins 1 and 2 play opposite roles in adipogenesis via reciprocal regulation of peroxisome proliferator-activated receptor {gamma}. J Biol Chem. 2011; 286:1354–1363. [PubMed: 21047783]

Petersen KF, Befroy D, Dufour S, Dziura J, Ariyan C, Rothman DL, DiPietro L, Cline GW, Shulman GI. Mitochondrial dysfunction in the elderly: possible role in insulin resistance. Science. 2003; 300:1140–1142. [PubMed: 12750520]

Reid IR. Fat and bone. Arch Biochem Biophys. 2010; 503:20–27. [PubMed: 20599663]

Sonoda J, Mehl IR, Chong LW, Nofsinger RR, Evans RM. PGC-1beta controls mitochondrial metabolism to modulate circadian activity, adaptive thermogenesis, and hepatic steatosis. Proc Natl Acad Sci USA. 2007; 104:5223–5228. [PubMed: 17360356]

Sottile V, Seuwen K, Kneissel M. Enhanced marrow adipogenesis and bone resorption in estrogen-deprived rats treated with the PPARgamma agonist BRL49653 (rosiglitazone). Calcif Tissue Int. 2004; 75:329–337. [PubMed: 15549648]

Tontonoz P, Spiegelman BM. Fat and beyond: the diverse biology of PPARgamma. Annu Rev Biochem. 2008; 77:289–312. [PubMed: 18518822]

van Beekum O, Fleskens V, Kalkhoven E. Posttranslational modifications of PPAR-gamma: fine-tuning the metabolic master regulator. Obesity (Silver Spring). 2009; 17:213–219. [PubMed: 19169221]

Vestergaard P. Discrepancies in bone mineral density and fracture risk in patients with type 1 and type 2 diabetes--a meta-analysis. Osteoporos Int. 2007; 18:427–444. [PubMed: 17068657]

Vianna CR, Huntgeburth M, Coppari R, Choi CS, Lin J, Krauss S, Barbatelli G, Tzameli I, Kim YB, Cinti S, Shulman GI, Spiegelman BM, Lowell BB. Hypomorphic mutation of PGC-1beta causes mitochondrial dysfunction and liver insulin resistance. Cell Metab. 2006; 4:453–464. [PubMed: 17141629]

Wan Y. PPARγ in bone homeostasis. Trends Endocrinol Metab. 2010; 21:722–728. [PubMed: 20863714]

Wan Y, Chong LW, Evans RM. PPAR-gamma regulates osteoclastogenesis in mice. Nat Med. 2007; 13:1496–1503. [PubMed: 18059282]

Wei W, Wang X, Yang M, Smith LC, Dechow PC, Sonoda J, Evans RM, Wan Y. PGC1beta mediates PPARgamma activation of osteoclastogenesis and rosiglitazone-induced bone loss. Cell Metab. 2010; 11:503–516. [PubMed: 20519122]

Yu C, Markan K, Temple KA, Deplewski D, Brady MJ, Cohen RN. The nuclear receptor corepressors NCoR and SMRT decrease peroxisome proliferator-activated receptor gamma transcriptional

activity and repress 3T3-L1 adipogenesis. J Biol Chem. 2005; 280:13600–13605. [PubMed: 15691842]

Zinman B, Haffner SM, Herman WH, Holman RR, Lachin JM, Kravitz BG, Paul G, Jones NP, Aftring RP, Viberti G, Kahn SE. Effect of rosiglitazone, metformin, and glyburide on bone biomarkers in patients with type 2 diabetes. J Clin Endocrinol Metab. 2010; 95:134–142. [PubMed: 19875477]

Highlights

- ASXL2-null mice are osteopetrotic, lipodystrophic and insulin resistant
- Attenuated osteoclastogenesis in ASXL2 KO mice reflects failure of PPARγ activation
- c-Fos and PGC1β differentially regulate osteoclast formation and function
- ASXL2 independently regulates skeletal and metabolic homeostasis eTOC

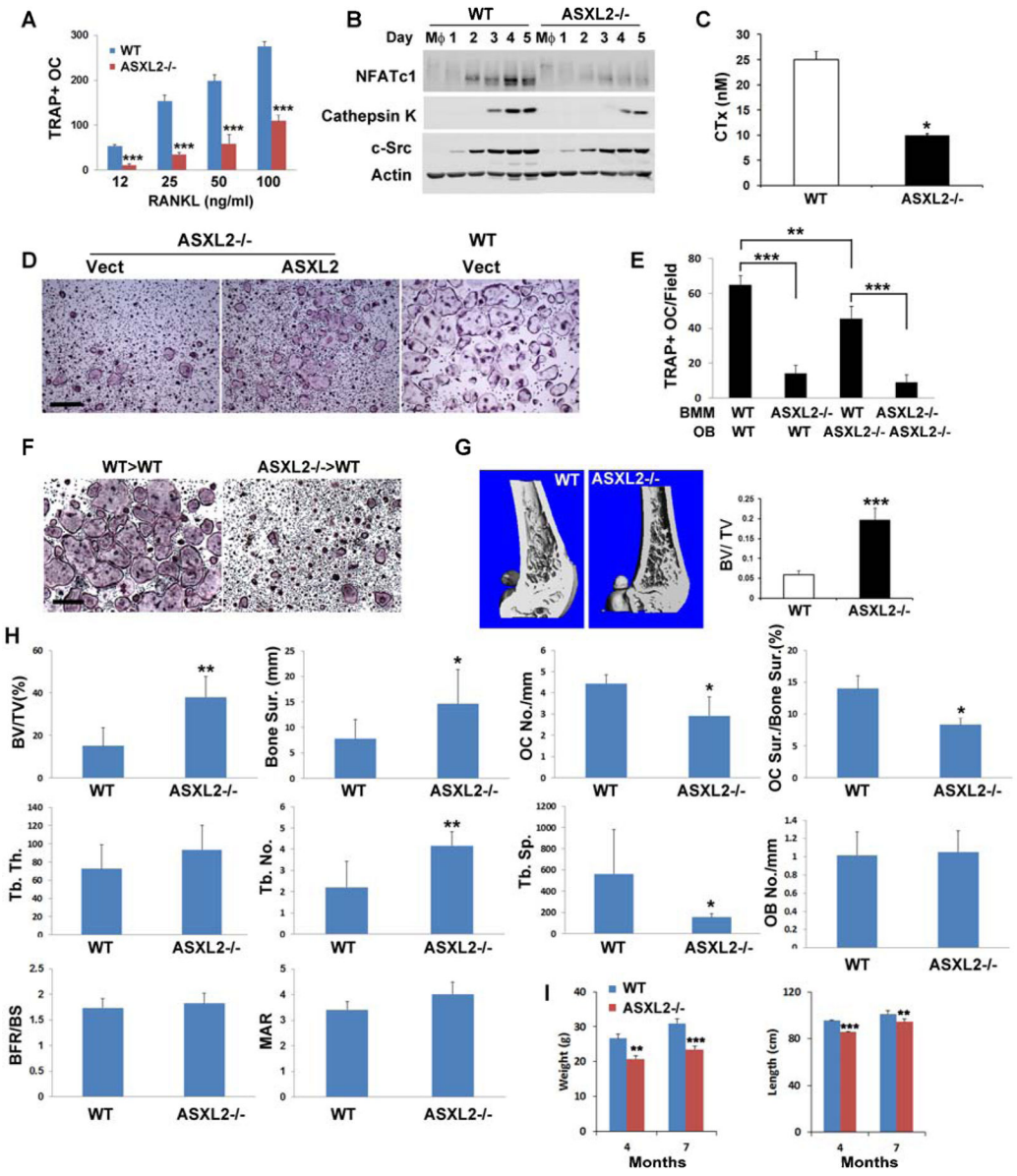

Fig 1.

ASXL2 deficiency results in impaired osteoclastogenesis. A) WT and ASXL2−/− BMMs were cultured with M-CSF and RANKL for 5 days and osteoclasts were counted. B) Osteoclast differentiation proteins were determined by immunoblot, with time. C) BMMs were cultured on bone with M-CSF and RANKL and medium CTx determined. D) ASXL2−/−BMMs, transduced with ASXL2 or vector, were exposed to M-CSF and RANKL for 5 days. The cells were TRAP stained. Vector-transduced WT cells serve as control. E) Various combinations of WT and ASXL2−/− BMMs and calvarial osteoblasts were co-cultured and osteoclasts were counted. F) WT or ASXL2−/− marrow was transplanted into irradiated WT hosts. Osteoclasts were generated from BMMs, ex vivo, 6 weeks after transplantation. G) Femurs of 13 wk old ASXL2−/− and WT littermates were subjected to μCT analysis and trabecular bone volume (BV/TV) determined. H) Static and dynamic

histomorphometric determination of trabecular bone of ASXL2−/− and WT mice. I) Weight and body length of WT and ASXL2−/− mice. Scale bar: 400 μm.

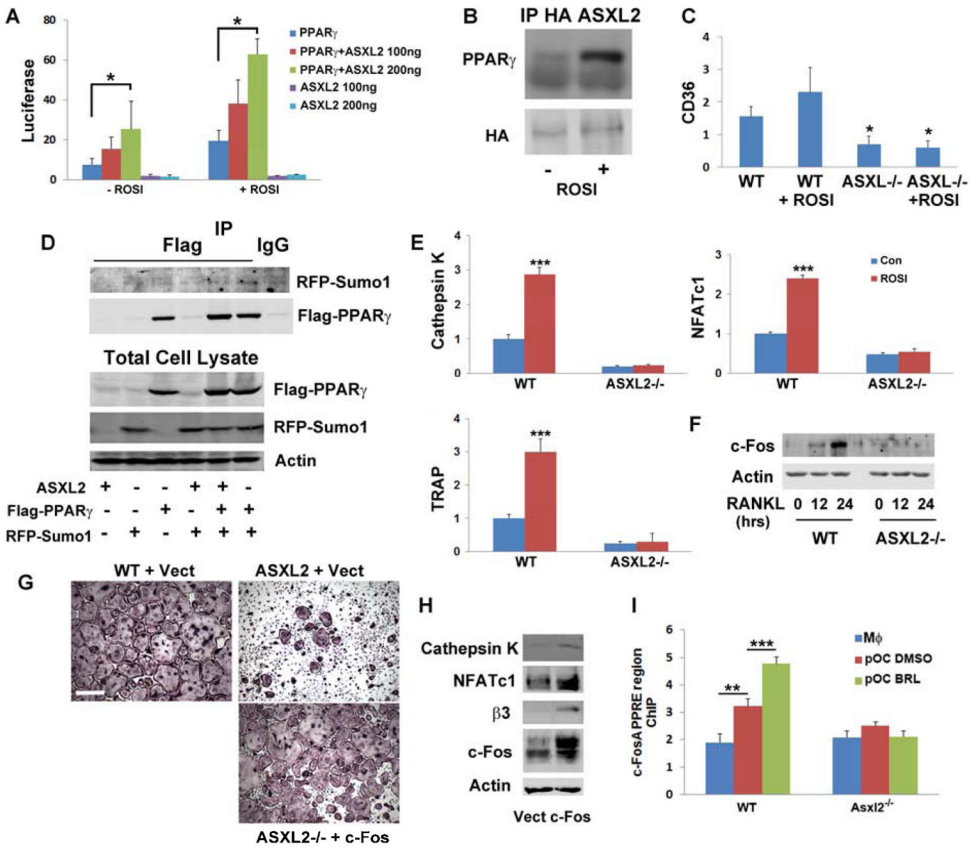

Fig 2.

ASXL2 mediates PPARγ stimulated osteoclastogenesis. A) PPARγ and/or ASXL2 were transfected into 293T cells containing a PPARγ luciferase reporter construct. The cells were treated with ROSI or carrier and luciferase activity determined. B) 293T cells, transfected with HA-ASXL2 and PPARγ, were exposed to ROSI or carrier. HA immunoprecipitates were immunoblotted for PPARγ. C) BMMs were cultured in the presence of M-CSF and RANKL with or without ROSI. After 5 days CD36 mRNA was determined by qPCR. D) 293T cells transfected with various combinations of RFP-SUMO 1, FLAG-PPARγ and ASXL2. FLAG immunoprecipitates were immunoblotted for FLAG and RFP. E) BMMs were exposed to M-CSF and RANKL +/− ROSI. After 5 days osteoclast differentiation marker were determined by qPCR. F) BMMs were exposed to M-CSF and RANKL with time. c-Fos protein was measured. G and H) ASXL2−/− BMMS, transduced with c-Fos or vector, were exposed to M-CSF and RANKL and (G) stained for TRAP activity. (H) Expression of osteoclast differentiation proteins were determined by immunoblot. I) BMMs were exposed to M-CSF and RANKL for 3 days with ROSI or carrier. PPARγ binding to its response element in the c-Fos promoter was determined by ChIP assay. Scale bar: 400 μm.

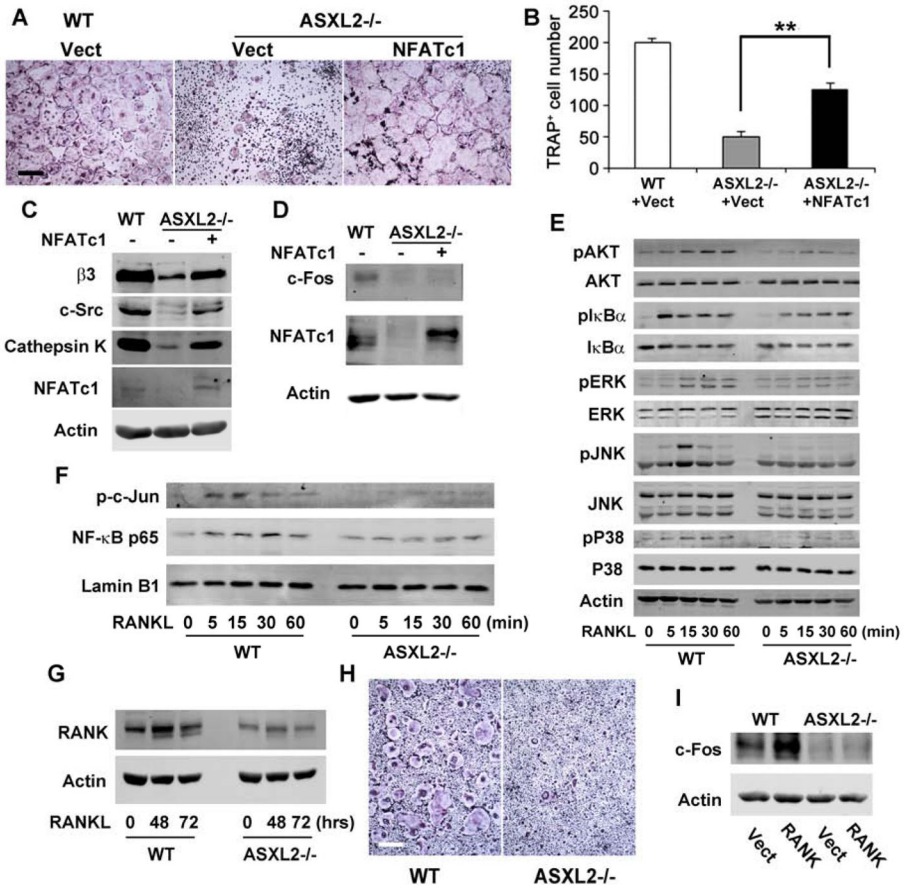

Fig 3.

RANK-stimulated osteoclast formation requires ASXL2. A,B,C) ASXL2−/− BMMS, transduced with NFATc1 or vector, were exposed to M-CSF and RANKL for 5 days. WT BMMs transduced with vector served as control. The cells were A) stained for TRAP; B) osteoclasts counted; C) Osteoclastogenic proteins were determined. D) ASXL2−/− BMMS, transduced with NFATc1 or vector were exposed to M-CSF and RANKL for 1 day. NFATc1 and c-Fos expression was determined. E and F) Cytokine/serum starved BMMs were exposed to RANKL with time. E) Cytoplasmic osteoclastogenic signaling molecule activation and F) nuclear osteoclastogenic signaling molecule activation were determined by immunoblot. G) BMMs were maintained in M-CSF alone for 3 days (0) or M-CSF and RANKL for 48 or 72 hrs. RANK protein was measured. H) BMMs, transduced with hFas/RANK, were exposed to M-CSF and anti-Fas activating antibody for 5 days. The cells were stained for TRAP activity. I) c-Fos expression by WT and ASXL2−/− BMMs, transduced with hFas/RANK or vector and exposed to M-CSF and anti-Fas activating antibody, was determined. Scale Bar: 400 μm.

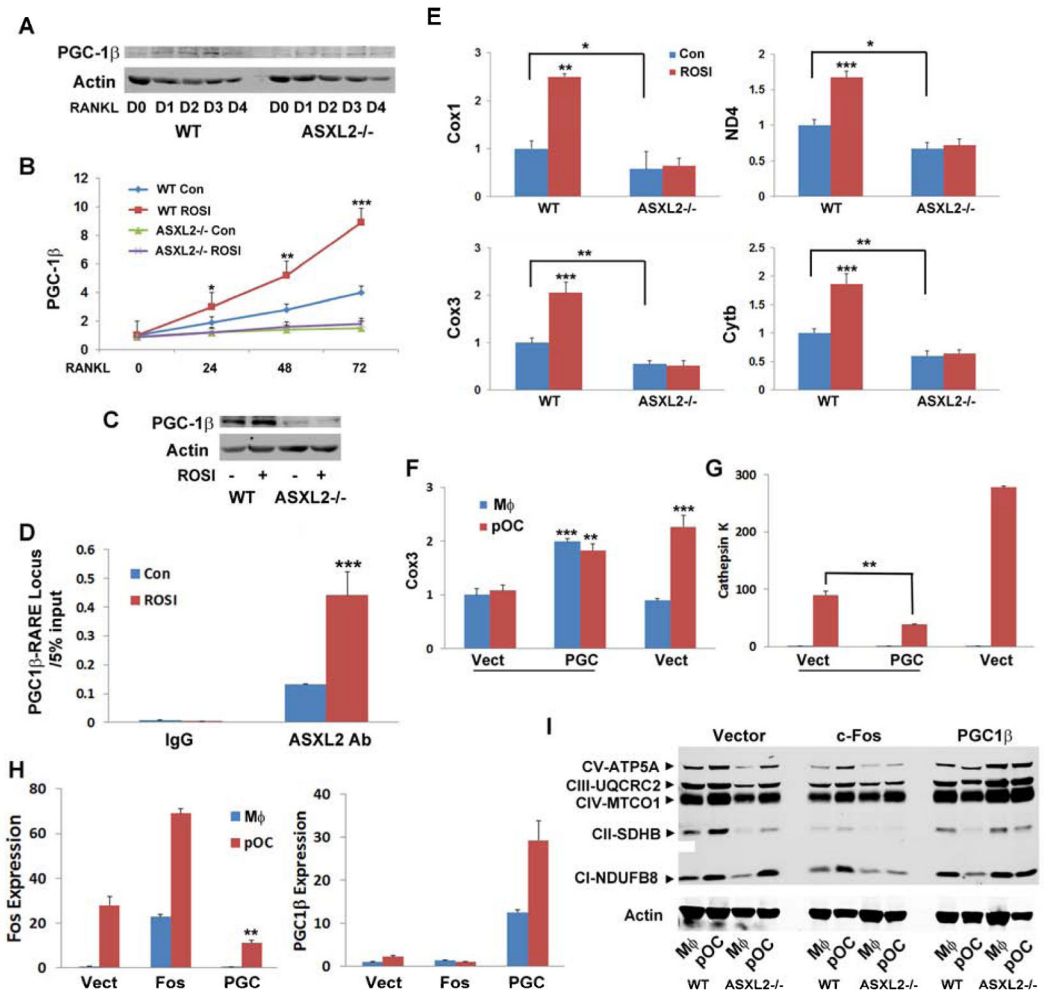

Fig 4.

ASXL2 promotes PGC-1β expression. A) BMMs were maintained in M-CSF and RANKL. PGC-1β was temporally measured by immunoblot. B,C) BMMs were maintained in M-CSF and RANKL +/− ROSI or carrier. PGC-1β B) mRNA and C) protein were measured by qPCR and immunoblot, respectively. D,E) BMMs were maintained in M-CSF and RANKL +/− ROSI or carrier for 3 days. (D) ASXL2 binding to the retinoic acid response element in the PGC-1β promoter was determined by ChIP assay. (E) Mitochondrial enzyme mRNAs were measured by qPCR. F,G) ASXL2−/− BMMs, transduced with PGC-1β or vector were maintained in M-CSF without (Mφ) or with RANKL (pOC) for 3 days. (F) Mitochondrial enzyme (Cox3). (G) Cathepsin K mRNA was measured by qPCR. Vector bearing WT cells serve as control. H) ASXL2−/− BMMs transduced with PGC-1β, c-Fos or vector were maintained in M-CSF without (Mφ) or with RANKL (pOC) for 3 days. c-Fos and PGC-1β mRNAs were determined by qPCR. Vector-bearing ASXL2−/− BMMs serve as control. I) Immunoblot of mitochondrial respiratory chain subunits (complexes I-V) expressed by BMMs and pOC derived from WT and ASXL2−/− mice transduced with vector, c-Fos or PGC-1β.

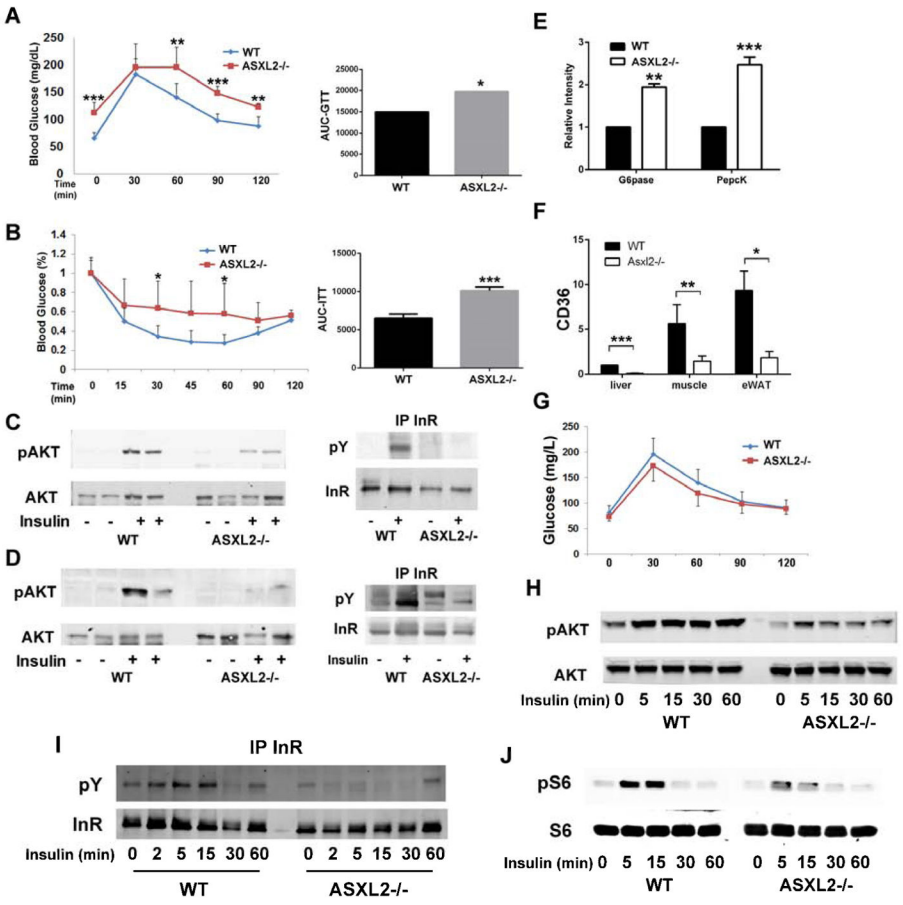

Fig 5.

ASXL2 regulates glucose and insulin sensitivity. A) Glucose tolerance test and its area under the curve of WT and ASXL2−/− mice. B) Insulin tolerance test and its area under the curve of WT and ASXL2−/− mice. C,D) WT and ASXL2−/− mice were injected with insulin (5U/Kg) or PBS. 10 min later phosphorylation of Akt and the insulin receptor was determined by immunoblot in (C) liver and (D) gastrocnemius muscle. E) Glucose-6-phosphatase (G-6-Pase) and phosphoenolpyruvate carboxykinase (Pepck) mRNA was measured by qPCR in WT and ASXL2−/− liver. F) CD36 mRNA expression by liver, muscle and epididymal white adipose tissue (eWAT) as determined by qPCR. G) Irradiated WT mice were transplanted with WT or ASXL2−/− marrow. 6 weeks later the animals were subjected to glucose tolerance tests. H,I,J) WT and ASXL2−/− BMMs were exposed to insulin. Phosphorylated H) AKT, I) insulin receptor and J) S6 were determined by immunoblot.

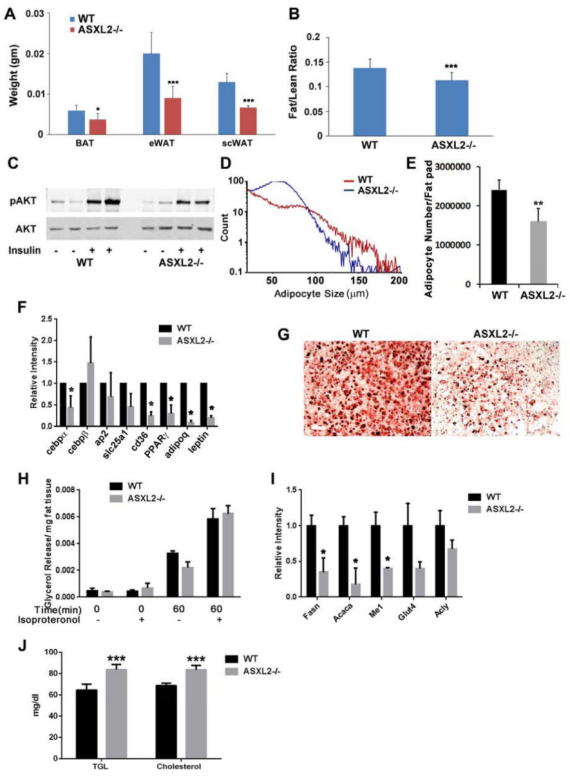

Fig 6.

ASXL2−/− mice are lipodystrophic. A) Weight of BAT, eWAT and scWAT in WT and ASLX2−/− mice. B) Fat/Lean ratio of WT and ASXL−/− mice. C) WT and ASXL2−/− mice were injected with insulin (5U/Kg) or PBS. 10 min later phosphorylation of Akt in epididymal fat was determined by immunoblot. D) WT and ASXL2−/− adipocyte size measured by osmium tetroxide staining. E) Adipocyte number in WT and ASXL2−/− epididymal fat pad. F) mRNA of adipogenic genes in ASXL2−/− and WT eWAT was measured by qPCR. G) Marrow stromal cells of WT and ASXL2−/− mice were cultured in adipogenic conditions for 14 days. The cells were stained with oil red O (red reaction product) to identify lipid. H) eWAT was treated with DMSO or isoproterenol for 1 h. Media glycerol content was determined. I) mRNA of lipid storage genes in WT and ASXL2−/− eWAT was measured by qPCR. J) Serum triglycerides and cholesterol of chow-fed WT and ASXL2−/− mice. Scale Bar: 50 μm.

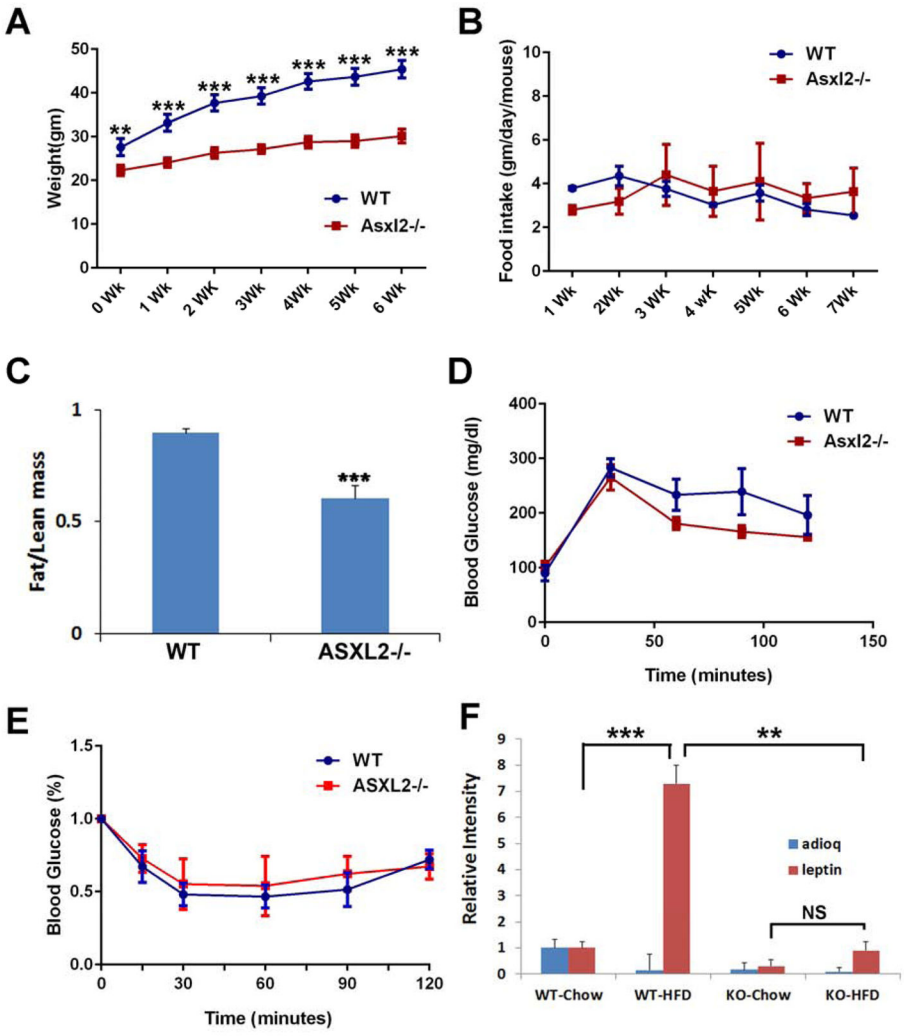

Fig 7.

ASXL2-deficient mice resist high fat diet. A-F) WT and ASXL2−/− mice were maintained on HFD for 7 weeks. A) Body weight. B) Weekly food intake. C) Fat/lean ratio as determined by DXA. D) Glucose tolerance test E) Insulin tolerance test. F) Adiponectin and leptin content in eWAT.